JOURNAL OF BACTERIOLOGY, Mar. 1978, p. 1053-1061
0021-9193/78/0133-1053$02.00/0

Vol. 133, No. 3
Printed in U.S.A.

DNA Replication Pattern and Cell Wall Growth in *Escherichia coli* PAT 84

LUUD J. H. KOPPES, NICO OVERBEEKE, AND NANNE NANNINGA*

Department of Electron Microscopy and Molecular Cytology, University of Amsterdam, Amsterdam, The Netherlands

Received for publication 30 August 1977

An electron microscopic radioautographic study was made of tritiated thymidine incorporation into the genome of *Escherichia coli* PAT 84 and of tritiated *meso*-D,L-2,6-diaminopimelic acid (DAP) into the cell envelope. Pulse-labeled cells growing at 30°C with a doubling time of 170 min were classified according to length by the method of agar filtration. Mathematical analysis of the length distribution led to the assumption of an exponential relation between length and time. A novel DNA replication pattern was found. Within the cell cycle DNA replication terminates at 70 min; then a gap follows of 64 min, after which DNA replication is initiated at 134 min. Thus, the *C* period is 106 min and the *D* period is 100 min. Cell constriction starts at 141 min and coincides with initiation of DNA replication. Detailed quantitative analysis of the [^{3}H]thymidine grain frequency distribution allowed the distinction of three groups of cells. The first group incorporated no label, the second group an amount *C*, and the third group an amount $2 \times C$. The relative contribution of each group to a particular length class was determined. The data fitted very well into the DNA replication pattern. The same analysis was carried out on DAP pulse-labeled cells. Again, three groups of cells could be distinguished, and their relative contributions to each length class was determined. The group with the double amount of label was especially prominent at the end of the cell cycle. The emergence of this group might represent the acquisition of new lateral growth areas.

During the cell cycle cells double their mass and duplicate their genomes before division restores the original situation. In rod-shaped bacteria such as *Escherichia coli*, this requires an understanding of how cells increase in length and how growth is correlated with events of the DNA replication cycle. Growth in length pertains especially to growth of the cell envelope layers. In *E. coli* this applies to the cell membrane (1), the peptidoglycan layer (17, 21, 23), and the outer membrane (19). Little is known about the expected coordination of the growth patterns of the respective layers. Even the growth pattern of one particular layer is insufficiently understood.

Growth of the peptidoglycan layer is considered to be zonal and not diffuse. This notion was based on radioautographic experiments with [^{3}H]*meso*-DL-2,6-diaminopimelic acid (DAP) pulse-labeled sacculi of various *E. coli* strains (17, 21). One zone was found in the central area of the cell and was assumed to be mainly involved in cell division; others are assumed to be involved in cell elongation (21). These results have recently been complemented by data on the localization of ampicillin-sensitive sites in *E. coli* B/r ATCC 12407 (23).

With respect to DNA replication and cell growth (and division), growth conditions have generally been chosen such that the timing of termination of DNA replication comes close to the onset of division (4, 9). Termination requires protein synthesis (15), and a terminal gene product is supposed to be involved in cell division (10). It has been shown that the nucleoplasmic bodies are separated upon termination (25), and for topological reasons it is clear that nucleoplasmic separation has to occur before division can be completed. Several processes show a different activity towards the end of the cell cycle. In synchronized *E. coli* (doubling time, 45 min) an increase in rate of murein synthesis (9) and in the incorporation of proteins and lipids into cell wall has been observed (4). In this particular case it was not clear whether these phenomena coincide in time with the initiation of DNA replication, termination of DNA replication, or cell division.

In this paper we present a radioautographic study of tritiated thymidine and DAP incorporation into *E. coli* PAT 84. The doubling time (τ = 170 min) has been chosen in such a way that, on the one hand, initiation of DNA replication and termination of DNA replication, and,

on the other hand, termination of DNA replication and the onset of division are well separated in time.

MATERIALS AND METHODS

Bacterial strain and growth condition. *E. coli* PAT 84 (F^- *thr leu thy his arg trp xyl mtl lac dap lys ftsA* T84) was obtained from U. Schwarz, Tübingen, Germany. Cells were grown aerobically with shaking at 30°C with a doubling time $\tau = 170$ min. The growth medium contained, per liter of twice-distilled water: 0.2 g of $MgSO_4 \cdot 7H_2O$, 2 g of citric acid, 10 g of K_2HPO_4, and 3.5 g of $NaNH_4PO_4 \cdot 4H_2O$, supplemented with 50 μg of thymine/ml, 20 μg of lysine/ml, 20 μg of DAP/ml, and 0.1% Casamino Acids (Difco Laboratories, Detroit, Mich.). Balanced growth was verified by obtaining a constant mass-to-cell ratio and by obtaining the same length distributions in two consecutive samples. Mass was measured as optical density at 450 nm with a Gilford microsample spectrophotometer. Cell number was counted with a Coulter counter model Z_B (aperture diameter, 30 μm). Length distributions were made of cells prepared by agar filtration (25, 26).

Labeling with [^{3}H]thymidine. Cells were grown in 50 ml of medium to a density of about 5×10^7 cells/ml. They were poured on a filter (pore size, 0.45 μm; Millipore Corp., Bedford, Mass.), washed with prewarmed medium without thymine, and then resuspended in 40 ml of thymine-free medium. [^{3}H]thymidine was obtained from Radiochemical Centre, Amersham, England (1 mCi/ml; specific activity, 45 Ci/mmol). After addition of 1 ml of cell suspension to 20 μl of [^{3}H]thymidine (final concentration, 0.08 μg of thymidine/ml), radioactivity of 50-μl samples taken at successive times was determined. The samples were collected on filter disks (Millipore Corp.) and washed with 20 ml of ice-cold trichloroacetic acid (10%, wt/vol) and then with 10 ml of ice-cold 5% trichloroacetic acid. The filter disks were dried and placed in scintillation vials containing 5 ml of toluene-2,5-diphenyloxazole (PPO) and 1,4-bis-[2]-(5-phenyloxazolyl)benzene (POPOP). The samples were counted in a Nuclear-Chicago liquid scintillation counter (ISOCAP/300). Pulse labeling for radioautography was carried out for 10 min. The reaction was stopped by placing 1-ml samples on ice and then adding successively 4 ml of ice-cold growth medium supplemented with 1 mg of thymidine/ml and 1 ml of 1% (wt/vol) ice-cold OsO_4 in R-K-buffer (18). After 30 min samples were filtered (pore size, 0.45 μm; Millipore Corp.) and washed with 50 ml of buffer containing: 10 mM tris(hydroxymethyl)-aminomethane-acetic acid (pH 7.4), 1 mM $MgCl_2$, and 0.5 mg of thymidine/ml. Finally, cells were resuspended in 1 ml of growth medium with 0.05 M NaN_3 and 0.1% OsO_4 and prepared for electron microscopy by the method of agar filtration (26).

Labeling with [^{3}H]DAP. The radioisotope was from CEA, Gif-sur-Yvette, France (2 mCi/ml; specific activity, 45 Ci/mmol). Amounts of 1 ml of cell suspension (without DAP) were added directly or after 15 min (DAP starvation) to 10 μl of [^{3}H]DAP (final concentration, 0.08 μg of DAP/ml). The pulse duration was 20 min.

Radioautography. The plastic film (with adhering bacteria) prepared by agar filtration was floated off on distilled water. It was picked up from below with a glass slide, previously covered with a collodion membrane. The slides were dipped in Ilford L4 emulsion, diluted with 2 volumes of distilled water at 32°C with a semiautomatic apparatus (12). Controls were looked at immediately in an electron microscope to check whether the emulsion was present as a monolayer. After exposure for 10 days, the slides were developed for 7 min in Agfa-Gevaert developer. Development of the preparation of cells pulse labeled with [^{3}H]DAP was preceded with 1 min of gold latensification (13). The radioautograms were transferred to electron microscope grids, and areas were photographed at random with a Philips EM 300 electron microscope. The radioautographic resolution of the technique was assessed from the distribution of grains lying above the cell constriction of [^{3}H]DAP pulse-labeled cells. A plot of the cumulative frequency of grains versus distance to the site of constriction gave a half-distance (HD) value of 0.32 μm (for HD estimates, see 20). This value is an overestimate; because the radioactive source is not exclusively located in the constriction site, the value will be smaller. To analyze the topography of grains, 0.25 μm was chosen as a width for the zones into which the [^{3}H]DAP pulse-labeled cells were divided. For the analysis of radioautographs, the cell length of cells was measured, and the overlying grains were counted from projections of the negative on a transparent screen at a final magnification of 12,000 × ([^{3}H]DAP pulse-labeled cells).

RESULTS

Relationship between length and time. Since in our approach cells are classified according to length, it is relevant to assess whether the relationship between length and time is, for instance, linear or exponential. Therefore, the Collins and Richmond principle (2) was applied to the length distribution shown in Fig. 1A. This principle allows the calculation of the average rate of elongation of individual cells in a steady-state culture from the length distributions of extant, newborn, and separating cells. The length distribution was obtained as follows. The cumulative length distributions (not shown) of untreated cells fixed at 3 h before pulse labeling and of cells covered with emulsion after pulse labeling with [^{3}H]thymidine for 0 and 10 min differed only slightly according to the Kolmogorov-Smirnov test (22). With the 0-min-pulse cells taken as reference, the maximal observed differences of the unlabeled cells and cells labeled for 10 min were 10.0 and 5.5%, respectively. The values allowed by chance (with a level of significance $\alpha = 0.01$) were 10.4 and 9.7%. Length measurements of the three groups of cells were pooled to construct the length distribution in Fig. 1A. Also indicated (speckled area) is the distribution of constricting cells (12.4% of the total population).

The length distributions of newborn cells and

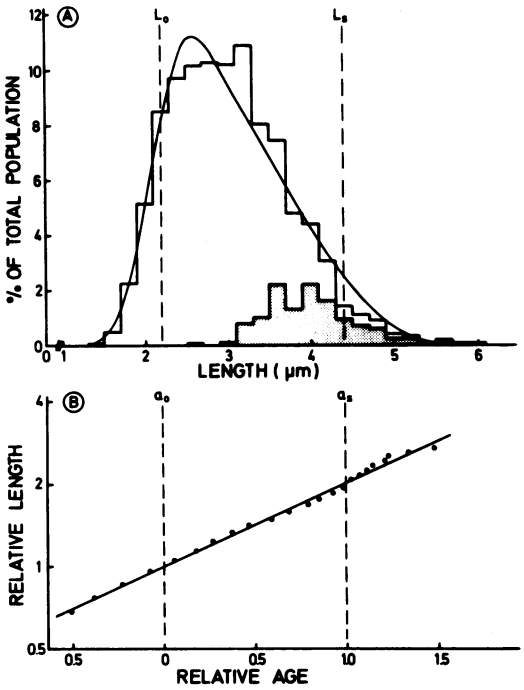

FIG. 1. *Length distribution and growth kinetics of E. coli PAT 84. (A) Length distribution of E. coli PAT 84 prepared by agar filtration (histogram). Length measurements of untreated cells (N = 503) and of cells labeled with [^{3}H]thymidine for 0 min (N = 476) and for 10 min (N = 697) and subsequently covered with emulsion have been combined. The average length of the cells is 3.04 μm; the coefficient of variation (CV) is 23.5%. The speckled area represents the distribution of dividing (constricting) cells (N = 207); the average length is 4.02 μm; the CV = 13.5%. The average lengths of the newborn cell (L_0 = 2.2 μm) and of the separating cell (L_s = 4.4 μm) have been determined according to Harvey et al. (6). (B) Semilog plot of length of individual cells versus relative age. The average rate of elongation in each length class was calculated with the formula of Collins and Richmond (2) from the measured length distribution of extant cells and from the estimated distributions of newborn and separating cells. The distributions of separating and newborn cells were assumed to be normal with CVs equal to that of the constricting cells (13.5%) and daughters of the constricting cells (14.4%), respectively. The age of a cell at a particular length relative to the age a_0 at length L_0 was obtained by integrating the reciprocal of the rate of elongation over intermediate lengths (6). Length and age are represented in arbitrary units: one unit of length is equal to L_0 = 2.2 μm; one unit of age is equal to τ = 170 min; a_s represents the age at cell separation. The straight line was obtained by linear regression. From this line the length distribution was recalculated (continuous line in Fig. 1A).*

of separating cells were assumed to be normal. The average lengths of the newborn cell, L_0, and the separating cell, L_s, were derived according to Harvey et al. (6) and are indicated in Fig. 1A. The coefficient of variation (CV) of length at cell separation (L_s) and birth (L_0) was assumed to be equal to that of the length distribution of constricting cells and the daughters of the constricting cells, respectively.

For each length class the average rate of cell elongation was calculated, and the average age of each length class was calculated by integrating the reciprocal of the rate of elongation over the shorter cell lengths (6). It will be appreciated from Fig. 1B that the relationship between length and time is largely exponential. A deviation occurs at the end of the cell cycle. From the straight line drawn through the points in Fig. 1B, the length distribution has been recalculated (continuous line in Fig. 1A). The maximal observed difference between the cumulative theoretical and experimental distributions was 3.4%; that allowed by chance (α = 0.01) was 4.0%.

DNA replication cycle. The location of the DNA replication period within the cell cycle was determined by whole-mount radioautography. Based on the kinetics of the incorporation of [^{3}H]thymidine into acid-precipitable material (result not shown), a pulse of 10 min was considered to be sufficient. Cells were classified according to length, and the percentage of labeled cells per length class was determined (Fig. 2). It can be observed that a DNA synthesis-less gap occurs between periods of DNA synthesis at the beginning and at the end of the cell cycle. This will be further analyzed below.

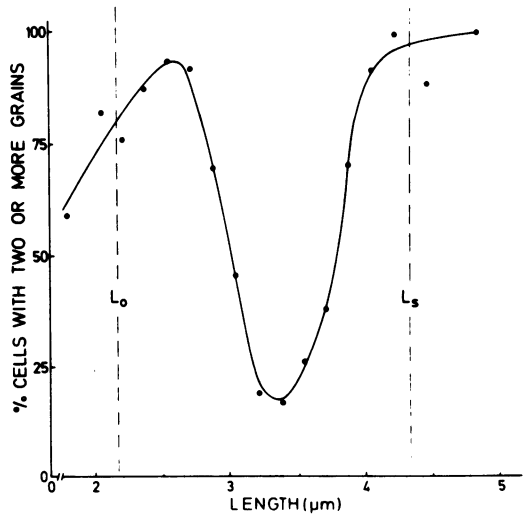

FIG. 2. *DNA replication cycle. The percentage of cells with more than one grain per cell is shown for 17 length classes. The control (pulse stopped at zero time) contained less than 0.1 grain per cell. Also indicated are L_0 and L_s which were taken from Fig. 1.*

Rate of DNA synthesis. In Fig. 3 the number of silver grains (n) is plotted against the frequency function $H(n)$. If all cells have incorporated the same amount of radioactivity in their DNA, the number of grains per cell (n) should follow the Poisson law [$P(n) = e^z \cdot z^n/n!$, where $P(n)$ is the fraction of cells with n grains and z is the average number of grains]. Plotting the frequency function $H(n) = \ln [P(n) \cdot n!]$ versus n should result in a straight line with a slope equal to ln z and a y axis intercept equal to $-z$ (see 5). Deviation from a straight line, when plotting the function $H(n)$ versus n, indicates different amounts of label incorporated by the cells during pulse labeling. As can be seen from Fig. 3, the latter situation is found. Without assumptions, we could divide the curve of Fig. 3 into three portions: (i) a zero group with 0.35 grain per cell (G), i.e., cells that did not incorporate label; (ii) a group with 5.15 grains per cell (C); and (iii) a group with 2 × 5.15 grains per cell ($2C$). The contribution of each group per length class has been calculated (see Appendix), and the results are shown in Fig. 4. It can be seen that the zero group dominates during the gap in DNA synthesis, that the C group occurs at the beginning of the cell cycle, and that the $2C$ group occurs at the end of the cell cycle. It will be appreciated from Fig. 2 that this is not unexpected; a new replication cycle starts some time before division. During this period the cell contains a double number of replication forks. For this reason, we consider the above approach justified. As will become clear below, this conclusion is relevant for the interpretation of the DAP-incorporation experiments.

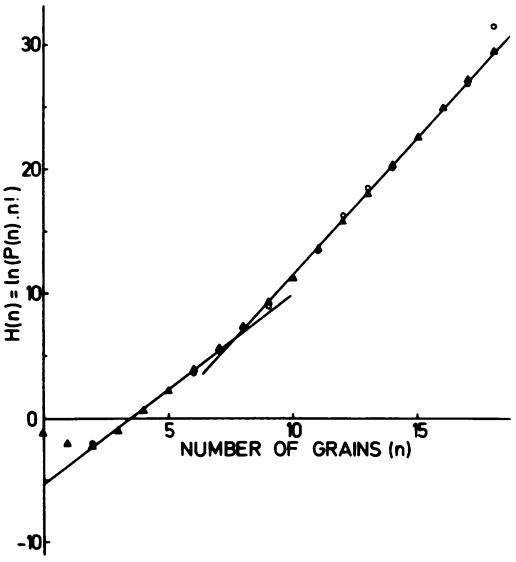

FIG. 3. *[^{3}H]thymidine grain frequency distribution. Plot of $H(n) = \ln[P(n) \cdot n!]$ versus n, where n is the number of grains over a cell and P(n) is the probability of observing a cell with n grains in the labeled population (see 5).* (○) *Observed distribution of grain counts;* (▲) *best fit to the observed distribution calculated by computer on the following assumptions: (i) the population is composed of three subpopulations with (a) a low average grain count G, consistent with cells not synthesizing DNA during the pulse, (b) an average grain count C, consistent with cells synthesizing DNA, and (c) an average grain count 2C, consistent with cells with twofold DNA synthesizing activity; and (ii) the grain counts in each subpopulation are distributed according to the Poisson law. The values of G, C, and 2C found for the best fit were, respectively, G = 0.35 grain/cell (SD = 0.14) for 40% of the population, C = 5.15 grains/cell (SD = 0.48) for 46% of the population, and 2C = 10.30 grains/cell (SD = 0.96) for 14% of the population. Where open circles and closed triangles coincide, only the latter are shown. For details of the computer program see Appendix.*

[^{3}H]DAP incorporation. Since peptidoglycan precursors move from the cytoplasm via the cell membrane into the sacculus (after the necessary modifications), we wanted to preserve the cell as intact as feasible, i.e., to keep the cell membrane in its original proximity to the cell wall. This was achieved by fixation with osmium tetroxide, which at the same time makes the cells leaky by destruction of the permeability barrier (24).

The kinetics of [^{3}H]DAP incorporation (Fig. 5) suggested to us to grow the cells for some time without DAP before administration of the pulse. To check whether the population changes upon starvation, the cumulative length distribution of the DAP-starved cells was compared with the cumulative length distribution derived from Fig. 1A (not shown). The maximal difference was 9.0%, whereas 8.5% is allowed for a level of significance of $\alpha = 0.01$ (22); however, we do not expect this small difference to have any major influence on our results. Radioautographs of pulse-labeled cells were analyzed with respect to the number of grains per cell in nine length classes (Fig. 6). The same overall result was obtained by analysis of radioautographs of isolated sacculi by Ryter et al. (17), i.e., the largest cells have about two times as many grains as the smallest ones.

Quantitative analysis of DAP radioautographs. Further analysis was carried out as for the DNA replication cycle (see above). The number of grains plotted against the frequency function $H(n) = \ln [P(n) \cdot n!]$ is shown in Fig. 7. We did not find a straight line; this indicates that not all cells incorporate [^{3}H]DAP at the same rate. Again, we could divide the curve into three parts (see Appendix for details of the cal-

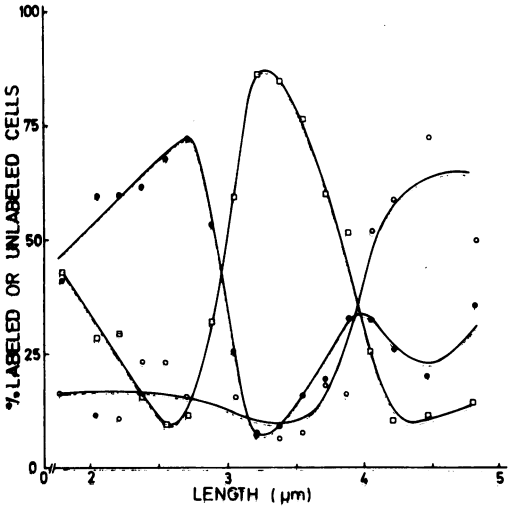

FIG. 4. *Contributions of the three groups with different average grain counts to each length class in the [³H]thymidine-labeled population (see Fig. 2). The calculation by computer was based on (i) the values of G, C, and 2C (see legend to Fig. 3) and (ii) the observed frequency distribution of grain number in each length class.* (□) *G;* (●) *C;* (○) *2C. For details see Appendix.*

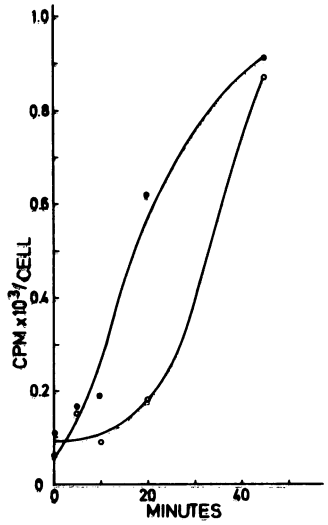

FIG. 5. *Incorporation of [³H]DAP into trichloroacetic acid-precipitable material. Label was added directly* (○) *or after growth for 15 min without DAP* (●).

culations): (i) a zero group (*G*) with 1.37 grains per cell, (ii) a group (*C*) with 6.47 grains per cell, and (iii) a group (2*C*) with 2 × 6.47 grains per cell. The contribution of each group to the various length classes is shown in Fig. 8. The zero group is largest at the beginning of the cell cycle (about 70%) and then levels off quickly to a final value of 20%. By contrast, the *C* group starts with about 20% and increases to a constant level of 40%; at the end of the cell cycle, it goes down again. The contribution of the 2*C* group is especially evident at the end of the cell cycle.

Topography of [³H]DAP incorporation. The position of 1,894 grains was measured as distance to the cell center for four groups of cellular length classes (Fig. 9). The data resemble previous observations (17, 21). In the smallest cells (Fig. 9a) no well-defined location of grains occurs, though there is an indication for polar location of some grains. The latter presumably arise from poles radioactively labeled when they were involved in division (17). In longer cells, cells are predominantly labeled in the cell center (Fig. 9b and c). In the longest cells (Fig. 9d), a shoulder appears, indicating the presence of label towards each side of the cell center.

DNA replication and cell length. The data of Fig. 4 were plotted on normal probability paper (Fig. 10). Assuming normal distributions for the lengths at initiation and termination of DNA replication, the average lengths and standard deviations at which these events occur can be obtained by linear regression. The length at which termination occurs has been determined in two ways: (i) by plotting the decreasing percentage of labeled cells (the group with 5.15 grains per cell) or (ii) by plotting the increasing percentage of unlabeled cells belonging to the group with 0.35 grain per cell (Fig. 4). In the first case an average termination length (L_{t1}) of 2.9 μm was found; in the second case L_{t2} was 3.0 μm. In both cases the standard deviation (SD) was 0.23 μm. Termination thus occurs at about t = 70 min (Fig. 10).

The average length at which DNA replication

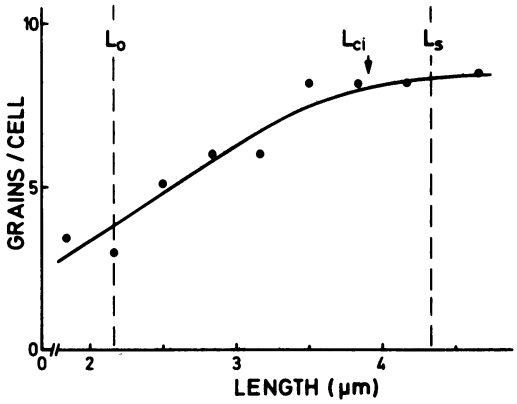

FIG. 6. *[³H]DAP incorporation during the cell cycle. The average number of grains per cell in each of the nine length classes is plotted. The control had less than 0.1 grain per cell. Also indicated are* L_0, L_s, *and* L_{ci} *taken from Fig. 1 and Fig. 10, respectively.*

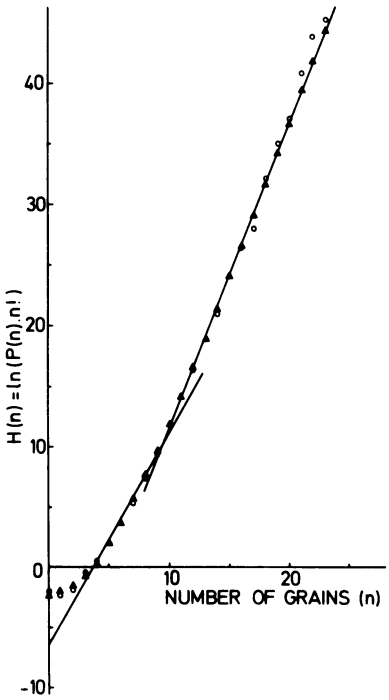

FIG. 7. *[^{3}H]DAP grain frequency distribution. Plot of H(n) = ln [P(n) · n!] versus n, where n is the number of grains over a cell and P(n) is the probability of observing a cell with n grains in the labeled population.* (○) *Observed distribution of grains;* (▲) *best fit to the observed distribution (see Fig. 3). The values of G, C, and 2C found for the best fit were, respectively: G = 1.37 grains/cell (SD = 0.26) for 38% of the population, C = 6.47 grains/cell (SD = 0.42) for 40% of the population, and 2C = 12.94 grains/cell (SD = 0.84) for 22% of the population. Where open circles and closed triangles coincide, only the latter are shown. For details see Appendix.*

starts (L_i) was determined from the zero-group cells (Fig. 4), i.e., from the decreasing percentage of unlabeled cells. L_i is 3.8 μm (SD = 0.37 μm) where t = 134 min (Fig. 10). The percentages of constricting cells per length class derived from Fig. 1A are likewise plotted in Fig. 10. A correction has been applied for cells that disappear because of division. To carry out this correction, a coefficient of variation of 13.5% has been assumed for the length of separating cells (see L. J. H. Koppes et al., in press). The average length at which constriction starts (L_{ci}) appeared to be 3.9 μm (SD = 0.58 μm), and the T period takes 29 min (170 − 141; Fig. 10). It can further be seen from Fig. 10 that L_t and L_{ci} are about 71 min apart, that DNA replication takes 106 min (C period), and that the D period (by definition the time between termination of DNA replication and cell division [7]) is 100 min. Note that the time scale is exponential.

DISCUSSION

DNA replication pattern. In slow-growing *E. coli* cells at least three replication cycles can be distinguished: (i) The most common pattern to this point is that in which initiation more or less coincides with division, and it occurs in *E. coli* B/r ATCC 12407 (3, 7) and *E. coli* K-12, 15,

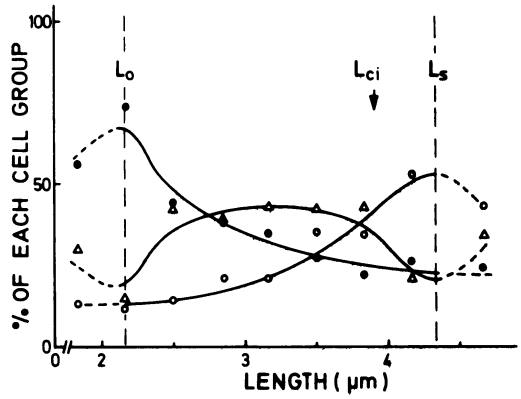

FIG. 8. *Contributions of the three groups with different average grain counts to the nine length classes in the [^{3}H]DAP pulse-labeled population. The calculation by computer was based upon the same assumptions as outlined in the legend to Fig. 4.* (●) *Contribution of the group with an average of 1.37 grains/cell to each length class,* (△) *the group with 6.47 grains/cell, and* (○) *the group with 12.94 grains/cell.*

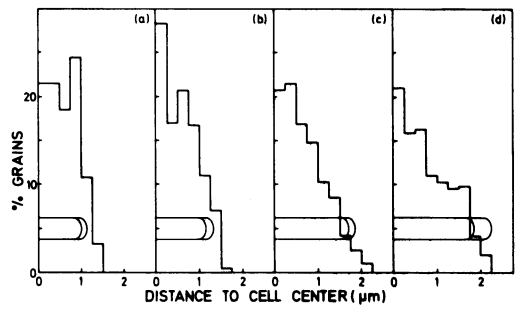

FIG. 9. *Topography of the grains in four length classes of the [^{3}H]DAP pulse-labeled population. The distance of the grains to the cell center was measured with a ruler on photographs printed at ×24,000 final magnification. Each cell half was divided into zones of equal width (0.25 μm). The percentage of the total grains in each zone was calculated and plotted in the histograms as a function of the distance to the cell center. In the lower part of each figure, the range of cell halves analyzed is indicated. (a) The distribution of 167 grains over 49 cells with lengths between 2.00 and 2.34 μm, (b) the distribution of 540 grains over 99 cells with lengths between 2.34 and 2.68 μm, (c) the distribution of 581 grains over 75 cells with lengths between 3.32 and 3.66 μm, and (d) the distribution of 606 grains over 74 cells with lengths between 3.66 and 4.34 μm.*

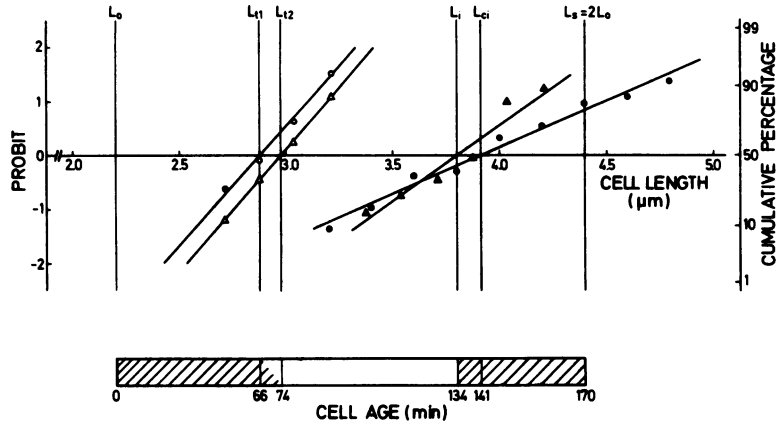

FIG. 10. *Contributions of the three groups with different average grain numbers to each length class in the [³H]thymidine pulse-labeled population (Fig. 4) replotted on probability paper to obtain the cumulative frequency distributions of termination (L_{t1} and L_{t2}) and initiation (L_i) of DNA replication and of initiation of cell constriction (L_{ci}) in the cell cycle of E. coli PAT 84. Assuming normal distribution of cell length at which the various events occur, average lengths (L) and standard deviations (SD) can be read directly from regression lines through the data points. The bar in the lower part of the figure represents a time scale based on the assumption of an exponential relation between cell length and average cell age (Fig. 1).* (△) *Percentage of cells per length class belonging to the group with G average grains per cell;* (○) *percentage of cells per length class belonging to the group with G or with 2C average grains per cell;* (▲) *percentage of cells per length class belonging to the group with C or with 2C average grains per cell;* (●) *percentage of constricted cells per length class corrected for the cells that have already disappeared by cell separation. For execution of the latter correction, the cumulative frequency distribution of separating cells must be known (Koppes et al., in press). This distribution was assumed to be normal with an average cell length (L_s) as determined by the method of Harvey et al. (6) and a coefficient of variation equal to that of the population of constricted cells (13.5%). For further explanation see text.*

15T⁻ (3). (ii) The case in which no DNA is synthesized at the beginning of the cell cycle applies to *E. coli* B/r K (8, 14) and *E. coli* B/r F 26 (8). (iii) The pattern in which replication starts at the end of the cell cycle and terminates in the next one occurs in *E. coli* PAT 84, and in this case the *D* period is very long (100 min).

In view of the unusually long *D* period of PAT 84, it is desirable to assess the reliability of the radioautographic method in determining the DNA replication pattern. Recently, we have determined by radioautography the DNA replication cycles of slow-growing *E. coli* B/r ATCC 12407, B/r K, and B/r F 26 (Koppes et al., in press). We could largely confirm the results which have been obtained for the same strains by biochemical methods (8). The peculiar DNA replication pattern observed for PAT 84 should, therefore, be correct. The presence of the small peak for the group of cells with 5.15 grains per cell at the end of the cell cycle (Fig. 4) suggests that within the cell the two genomes do not start replication simultaneously.

Growth pattern of the envelope. Taken in their entirety, our radioautographic data are similar to the observations of Schwarz and coworkers (17, 21). They found that during most of the cell cycle the label occurs in a broad central area, whereas at the end of the cycle lateral areas appear. These data resemble ours on the location of ampicillin-sensitive sites (23). The central area was thought to be responsible for septum formation and the lateral areas to be responsible for cell elongation (21). It should be stressed that we use the term area because at present we cannot judge whether growth in an area beside a constriction site is zonal or diffuse.

In the type of analysis carried out, it has been assumed that growth areas are symmetrically arranged around the cell center. In other words, the two cell halves have been supposed to be equivalent, but this is not necessarily so. We therefore carried out a detailed statistical analysis to test the symmetry (or asymmetry) of the grain distribution in *E. coli* W7 (R. W. H. Verwer et al., manuscript in preparation). The analysis showed that equivalence of the cell halves is a reasonable assumption.

It is clear that the group with 2×6.47 grains per cell is already present before cell constriction starts. From Fig. 4 and 8 it is not unreasonable to suggest that the emergence of the 2*C* group is related (in time) to segregation of DNA replication. This seems in accord with data from fast-growing cells (τ = 45 min) in which murein is synthesized at an increased rate (9), and the rate of incorporation of proteins and lipids into cell wall likewise increased about 15 to 20 min before

cell division (4). In the experiments of Hakenbeck and Messer (4), however, no distinction could be made between initiation and termination of DNA replication. A rather tentative interpretation would be the following. Upon termination two separate genomes are produced which acquire new positions in the cell during DNA segregation (Fig. 11). As DNA segregation continues and new rounds of DNA replication are initiated, more and more cells would acquire new growth areas (Fig. 8). Genome doubling and the new spatial orientation of the genomes with respect to the cell envelope could then be the trigger for new growth areas (beside the central one).

Coordination of cell cycle events. Recently, Koch (11) posed the question whether initiation of DNA replication regulates cell division. Since it may be assumed that in *E. coli* cell constriction is tightly coupled to cell separation, the question can be rephrased by asking whether the precision at which DNA replication is initiated affects the precision at which cell constriction starts. In our case the precision can be expressed as the variation in length at which a cell cycle event occurs. According to Koch (11), an event with a smaller (or equal) CV can influence a process which occurs with a larger (or equal) CV. L_i has an SD of 0.37 μm (Fig. 10). However, this applies to two genomes. Per genome, the SD is then $0.37 \times 0.5^{\frac{1}{2}}$ μm = 0.26 μm. The CV is thus $0.26/1.9 \times 100 = 13.7\%$. The CV for L_t = 7.9% (SD = 0.23 μm) and for L_{ci} = 14.8% (SD = 0.58 μm).

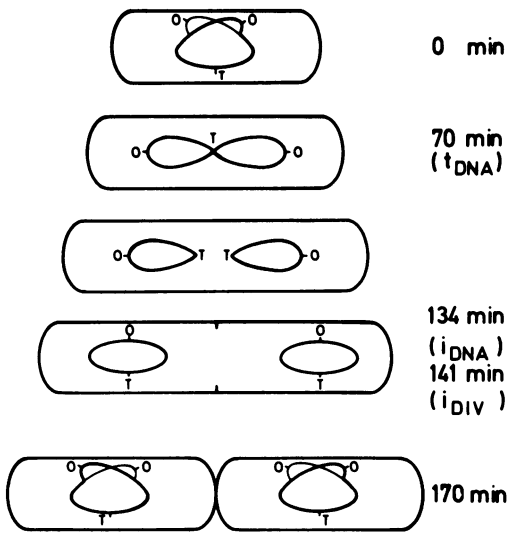

FIG. 11. *Scheme of the DNA replication cycle of E. coli PAT 84 (τ = 170 min). Note change of genome topology upon termination.*

The implication (following the reasoning of Koch [11]) is that initiation of DNA replication is slightly better controlled with respect to length than the onset of constriction (13.7 versus 14.8%). However, the matter is complicated by the fact that the two processes belong to different cell cycles, i.e., cell constriction to the present one and initiation of DNA replication to the next one. The same complication applies to termination and initiation. For the time being, therefore, it appears preferable to carry out such an analysis on more orthodox situations in which the DNA replication cycle is completed within one division cycle (Koppes et al., in press).

APPENDIX

Calculation of the best fit to the observed distribution of grains per cell in the combined length classes. By means of linear regression through selected points of the function $H(n) = \ln [P(n) \cdot n!]$, where n is the number of grains per cell and $P(n)$ is the observed fraction with n grains in the total population (see Fig. 3 and 7), two straight lines were obtained. From the slope and the y axis intercept of one of them, the average grain count (C') and contribution to the total population (S') for the group with the *lower* synthetic activity were estimated; from that of the other line, the average grain count (C'') and contribution to the total (T') for the group with the *higher* activity were estimated. If the pulse-labeled population is composed of three subpopulations with respective average numbers of grains per cell G, C, and $2C$ and with respective contributions to the total of $1 - (S + T)$, S, and T, and if grain numbers in each subpopulation follow the Poisson law, then the probability $P(n)$ of observing a cell with n grains is given by:

$$P(n) = (1 - S - T) \cdot e^{-G} \cdot G^n/n! + S \cdot e^{-C} \cdot C^n/n! + T \cdot e^{-2C} \cdot (2C)^n/n!$$

The computer systematically varied the four independent variables G, C, S, and T in the following manner: G from 0 up to 2 in steps of 0.2; C from $1/3(C' + C'') - 1$ up to $1/3(C' + C'') + 1$ in steps of 0.2; S from $S' - 0.1$ up to $S' + 0.1$ in steps of 0.02; and T from 0 up to $1 - S$ in steps of 0.02. For each combination of values placed on the four variables, the distribution function $P(n)$ was calculated according to the above formula and compared with the observed distribution by means of the Kolmogorov-Smirnov one-sample test of goodness of fit (22). When the calculated and observed distributions did not differ from each other with a level of significance of 0.10, the four parameters of the calculated distribution were stored in memory. After

all combinations of values for G, C, S, and T had been checked, the averages of those values stored were used in the calculation of the theoretical best-fit distribution, which is shown in the transformed form suggested by Hanawalt et al. (5) in Fig. 3 and 7.

Calculation of the contributions of the three groups with different activities to each individual length class. G and C in each length class were considered to be equal to that of the best fit found for the combined length classes (see above). The values of S and T were systematically varied: S from 0 up to 1 and T from 0 up to $1 - S$ in steps of 0.04. For each combination of S and T, a distribution was calculated according to the above formula and compared with the observed one in that length class by means of the Kolmogorov-Smirnov one-sample test of goodness of fit (22). When they did not differ with a level of significance of 0.10, the values for S and T were stored. After all combinations of values for S and T had been checked, the averages of the stored values were considered to be the contributions of the two synthetic groups to that length class.

ACKNOWLEDGMENTS

We have been much inspired by a paper of A. L. Koch (11). We thank G. J. Brakenhoff for his help with the computer and C. L. Woldringh for discussions. We also thank J. D. Leutscher for preparing the diagrams.

ADDENDUM IN PROOF

The Kolmogorov goodness-of-fit test is known to be conservative when the hypothesized distribution, like the Poisson distribution assumed above, is discontinuous. Therefore, calculated and observed distributions were also compared by means of the chi-square goodness-of-fit test with a level of significance of 0.05 (22). The values of G, C, S, and T found for the best fit were: $G = 0.34$ grain per cell (SD = 0.05), $C = 5.03$ grains per cell (SD = 0.15), $S = 0.45$ (SD = 0.02), and $T = 0.15$ (SD = 0.01). These values do not differ significantly from those found by means of the Kolmogorov test (see legend to Fig. 3). We thank R. W. H. Verwer for bringing this matter to our attention.

LITERATURE CITED

1. **Autissier, F., and A. Kepes.** 1971. Segregation of membrane during cell division in *Escherichia coli*. II. Segregation of Lac-permease and Mel-permease studied with a penicillin technique. Biochim. Biophys. Acta **249**:611–615.
2. **Collins, J. F., and M. H. Richmond.** 1962. Rate of growth of *Bacillus cereus* between divisions. J. Gen. Microbiol. **28**:15–33.
3. **Gudas, L. J., and A. B. Pardee.** 1974. Deoxyribonucleic acid synthesis during the division cycle of *Escherichia coli*: a comparison of strains B/r, K-12, 15, and 15T$^-$ under conditions of slow growth. J. Bacteriol. **117**:1216–1223.
4. **Hakenbeck, R., and W. Messer.** 1977. Oscillation in the synthesis of cell wall components in synchronized cultures of *Escherichia coli*. J. Bacteriol. **129**:1234–1238.
5. **Hanawalt, P. C., O. Maaløe, D. J. Cummings, and M. Schaechter.** 1961. The normal DNA replication cycle. II. J. Mol. Biol. **3**:156–165.
6. **Harvey, R. J., A. G. Marr, and P. R. Painter.** 1967. Kinetics of growth of individual cells of *Escherichia coli* and *Azotobacter agilis*. J. Bacteriol. **93**:605–617.
7. **Helmstetter, C. E., and S. Cooper.** 1968. DNA synthesis during the division cycle of rapidly growing *Escherichia coli* B/r. J. Mol. Biol. **31**:507–518.
8. **Helmstetter, C. H., and O. Pierucci.** 1976. DNA synthesis during the division cycle of three substrains of *Escherichia coli* B/r. J. Mol. Biol. **102**:477–486.
9. **Hoffmann, B., W. Messer, and U. Schwarz.** 1972. Regulation of polar cap formation in the life cycle of *Escherichia coli*. J. Supramol. Struct. **1**:29–37.
10. **Jones, N. C., and W. D. Donachie.** 1973. Chromosome replication, transcription and control of cell division in *Escherichia coli*. Nature (London) New Biol. **243**:100–103.
11. **Koch, A. L.** 1977. Does the initiation of chromosome replication regulate cell division? Adv. Microb. Physiol. **16**:49–98.
12. **Kopriwa, B. M.** 1973. A reliable, standardized technique for ultrastructural electron microscopic radioautography. Histochemie **37**:1–17.
13. **Kopriwa, B. M.** 1975. A comparison of various procedures for fine grain development in electron microscopic radioautography. Histochemistry **44**:201–224.
14. **Kubitschek, H. E., and M. L. Freedman.** 1971. Chromosome replication and the division cycle of *Escherichia coli* B/r. J. Bacteriol. **107**:95–99.
15. **Maranouchi, T., and W. Messer.** 1973. Replication of a specific terminal chromosome segment in *Escherichia coli* which is required for cell division. J. Mol. Biol. **78**:211–228.
16. **Pierucci, O.** 1972. Chromosome replication and cell division in *Escherichia coli* at various temperatures of growth. 1972. J. Bacteriol. **109**:848–854.
17. **Ryter, A., Y. Hirota, and U. Schwarz.** 1973. Process of cellular division in *Escherichia coli*. Growth pattern of *E. coli* murein. J. Mol. Biol. **78**:185–195.
18. **Ryter, A., E. Kellenberger, A. Birch-Andersen, and O. Maaløe.** 1958. Étude au microscope électronique de plasmas contenant de l'acide désoxyribonucléique. Les nucléoides des bactéries en croissance active. Z. Naturforsch. Teil B **13**:597–605.
19. **Ryter, A., H. Shuman, and M. Schwartz.** 1975. Integration of the receptor for bacteriophage lambda in the outer membrane of *Escherichia coli*: coupling with cell division. J. Bacteriol. **122**:295–301.
20. **Salpeter, M. M., L. Bachmann, and E. E. Salpeter.** 1969. Resolution in electron microscope radioautography. J. Cell. Biol. **41**:1–20.
21. **Schwarz, U., A. Ryter, A. Rambach, R. Hellio, and Y. Hirota.** 1975. Process of cellular division in *Escherichia coli*: differentiation of growth zones in the sacculus. J. Mol. Biol. **98**:749–760.
22. **Siegel, S.** 1956. Nonparametric statistics for the behavioural sciences. McGraw-Hill Kogakusha, Ltd., Tokyo.
23. **Staugaard, P., F. M. van den Berg, C. L. Woldringh, and N. Nanninga.** 1976. Localization of ampicillin-sensitive sites in *Escherichia coli* by electron microscopy. J. Bacteriol. **127**:1376–1381.
24. **Woldringh, C. L.** 1973. Effect of cations on the organization of the nucleoplasm in *Escherichia coli* prefixed with osmium tetroxide or glutaraldehyde. Cytobiologie **8**:97–111.
25. **Woldringh, C. L.** 1976. Morphological analysis of nuclear separation and cell division during the life cycle of *Escherichia coli*. J. Bacteriol. **125**:248–257.
26. **Woldringh, C. L., M. A. de Jong, W. van den Berg, and L. Koppes.** 1977. Morphological analysis of the division cycle of two *Escherichia coli* substrains during slow growth. J. Bacteriol. **131**:270–279.